INSTITUTE OF PHYSICS PUBLISHING PHYSICS IN MEDICINE AND BIOLOGY

Phys. Med. Biol. **47** (2002) N1–N10 PII: S0031-9155(02)29538-X

NOTE

Projection access order in algebraic reconstruction technique for diffuse optical tomography

Xavier Intes[1,2], Vasilis Ntziachristos[3], Joe P Culver[4], Arjun Yodh[2] and Britton Chance[1]

[1] Department of Biophysics and Biochemistry, University of Pennsylvania, Philadelphia, PA 19104, USA
[2] Department of Physics and Astronomy, University of Pennsylvania, Philadelphia, PA 19104, USA
[3] Center for Molecular Imaging Research, Massachusetts General Hospital and Harvard Medical School, Charlestown, MA 02129, USA
[4] NMR Center, Massachusetts General Hospital and Harvard Medical School, Charlestown, MA 02129, USA

E-mail: intes@mail.med.upenn.edu

Received 9 October 2001
Published 29 November 2001
Online at stacks.iop.org/PMB/47/N1

Abstract

Algebraic reconstruction technique (ART) is one of the popular image reconstruction techniques used in diffuse optical tomography (DOT). We investigate in this note the influence of the order in which data are accessed in ART. Simulations mimicking breast tissues in transmission geometry with contrast agent tumour enhancement were used to evaluate the image quality of the diverse projection access investigated. We show that by selecting proper projection access order, the convergence speed can be significantly improved when ART is used to perform DOT. Moreover, low-contrast detection is improved.

(Some figures in this article are in colour only in the electronic version)

1. Introduction

Diffuse optical tomography (DOT) is a new biomedical imaging modality that uses near infrared (NIR) light (Arridge 1999, Yodh and Chance 1995). In this spectral window, tissues exhibit low light absorption and the light propagation is governed predominantly by scattering. Thus, large volumes of tissues can be probed. Moreover, tissue-intrinsic absorption is principally due to oxy-haemoglobin and deoxy-haemoglobin. By retrieving the distributions of these two chromophores one is able to image tissue functional characteristics. Potential applications range from brain functional imaging (Villringer and Chance 1997) to cancer detection (Ntziachristos and Chance 2001, Hawrys and Sevick-Muraca 2000).

DOT employs measurements recorded from tissue using multiple optical source–detector pairs and retrieves (reconstructs) the targeted chromophore distribution by synthesizing the measurements through solution of an inverse problem. Similar to other tomographic approaches, such as x-ray computed tomography (CT), positron emission tomography (PET) or single photon emission computed tomography (SPECT), DOT first constructs the *forward problem*, which predicts the photon propagation for a known medium and then it *inverts* it.

A popular technique among the linear inversion techniques to resolve the inverse problem in this case is the algebraic reconstruction technique (ART) (Kak and Slaney 1987). This method is best suited for projections that are sparse, noisy or non-uniformly distributed and it has been successfully applied to DOT (O'Leary *et al* 1995, Ntziachristos *et al* 2000). Furthermore, it allows efficient processing of large inversion problems since it has minimum storage requirements and can be easily implemented with constraints such as object shape or non-negativity.

In this paper, we investigated three projection access-ordering schemes for DOT. In section 2, we discuss our methods including the choice of the algebraic technique, the model used for the forward operator, the generation of the dataset and finally the way we create the different access order. Section 3 presents reconstructions in slab geometry for the three access orders considered herein and the definition of the mathematical estimators used to assess the quality of the reconstructions. In section 4 we perform a discussion of the impact of the access order and the utility to consider a specific access order.

2. Methods

2.1. Forward model

The propagation of NIR light in tissue is well modelled by the diffusion equation. In the case of heterogeneity, the diffusion equation can be solved by a perturbative approach (O'Leary 1996). In this paper, we have used the Rytov approximation approach. In the case of DOT, multiple source–detector pairs are used. The media under consideration is sampled in voxels and the problem can be written as a matrix equation, i.e.

$$\begin{bmatrix} {}_{\mathrm{sc}}(r_{\mathrm{s}1}, r_{\mathrm{d}1}) \\ \vdots \\ {}_{\mathrm{sc}}(r_{\mathrm{s}m}, r_{\mathrm{d}m}) \end{bmatrix} = \begin{bmatrix} W_{11} & \dots & W_{1n} \\ \vdots & \ddots & \vdots \\ W_{m1} & \dots & W_{mn} \end{bmatrix} \begin{bmatrix} \delta\mu_{\mathrm{a}}(r_1) \\ \vdots \\ \delta\mu_{\mathrm{a}}(r_n) \end{bmatrix} \tag{1}$$

where ${}_{\mathrm{sc}}(r_{si}, r_{\mathrm{d}i})$ is the diffuse perturbative phase for the ith source–detector pair, W_{ij} (O'Leary 1996) is the weight for the jth voxel and the ith source–detector pair and $\delta\mu_a(r_j)$ is the differential absorption coefficient of the jth voxel. We limited our problem to image the absorption coefficient. Boundary conditions for semi-infinite geometries and slab geometries are derived using the extrapolated boundary condition and the image source technique (Haskell *et al* 1994).

2.2. Inversion using ART

Algebraic techniques are well known and broadly used in the biomedical community (Gordon *et al* 1970). ART solves a system of linear equations ($\mathbf{b} = \mathbf{Ax}$) by sequentially projecting a solution estimate onto the hyperplanes defined by each row of the linear system. The technique is used in an iterative scheme and the projection at the end of the kth iteration becomes the

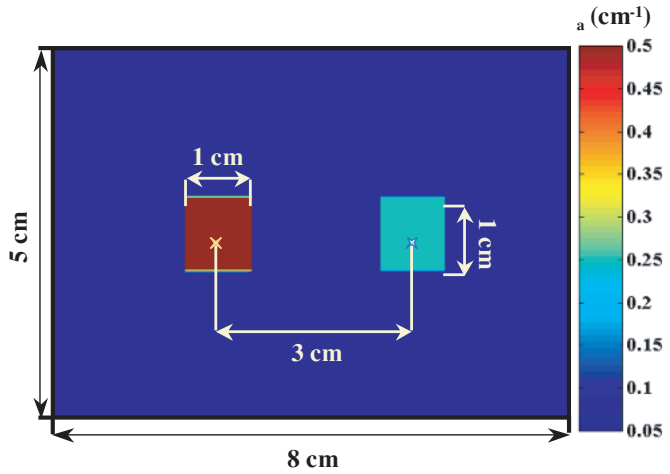

Figure 1. Model used for the simulations. The two objects have a contrast of 10 (object A) and 5 (object B) relative to the absorption background.

estimate for the $(k + 1)$th iteration. This projection process can be expressed mathematically as (Kak and Slaney 1987)

$$x_j^{(k+1)} = x_j^{(k)} + \lambda \frac{b_i - \sum_i a_{ij} x_j^{(k)}}{\sum_i a_{ij} a_{ij}} \sum_i a_{ij} \tag{2}$$

where $x_j^{(k)}$ is the kth estimate of jth element of the object function, b_i the ith measurement, a_{ij} the ijth element of the weight matrix $\mathbf{A}$ and λ the relaxation parameter.

The relaxation parameter adjusts the projection step for each iteration. The selection of λ is most of the time done empirically (Ros *et al* 1996, Herman and Meyer 1993, Gaudette *et al* 2000, van der Sluis and van der Vorst 1990). We have set $\lambda = 0.1$ based on previous studies with experimental data (Ntziachristos *et al* 2000).

2.3. Measurement generation

Measurements where obtained by solving the frequency-domain diffusion equation with a finite difference approach. We restricted our simulations to a two-dimensional (2D) geometry for computational efficiency.

The configuration we simulated in this study was a transmittance one which is a typical experimental configuration for NIR breast imaging (Ntziachristos *et al* 2000, Matson and Liu 2000, Culver *et al* 2000) as shown in figure 1.

The slab thickness was 5 cm. We placed 17 sources on one side of the slab and 257 detectors on the other side, both evenly stretched along 8 cm. The optical properties were chosen to mimic the average properties of the human breast (Durduran *et al* 2000): $\mu_{\mathrm{a}}^{\mathrm{background}} = 0.05\ \mathrm{cm}^{-1}$, $\mu_{\mathrm{s}}^{\mathrm{background}} = 10\ \mathrm{cm}^{-1}$. Two rectangular absorptive objects of 1 cm^2 were placed 3 cm apart in the centre of the slab. Those objects had a contrast of 10 (object A) and 5 (object B) relative to the absorption background.

The finite difference simulations used a $0.25 \times 0.25\ \mathrm{mm}^2$ grid size. All the simulations performed herein were realized at a 50 MHz frequency. A 1% random noise on amplitude and a 0.1° random noise on phase were added for all the simulations unless stated otherwise.

2.4. Access order

Different access orders have been proposed in the past. They all considered the classical case of a fan-beam configuration in CT to be assessed. The idea of these different access orders is to minimize the correlation between measurements b_i that are successively accessed by the iterative projection inversion method.

The goal is to prearrange the measurements in such a scheme that the projections are closest to perpendicularity. The different access order schemes proposed are the prime number decomposition (PND, Ros *et al* 1996), the random access scheme (RAS, van Dijke 1992), the multi-level scheme (MLS, Guan and Gordon 1994) and the weighted distance scheme (WDS, Mueller *et al* 1997). Those access orders are able to speed up the convergence rate of the ART and give better results in the first iteration relative to the sequential access scheme, which is the natural access order, i.e. access the projections in the order of the acquired experimental data. Moreover, they lead to better low-contrast detection (Guan *et al* 1998). They have demonstrated significant conversion improvement in CT, PET and SPECT.

In DOT, light undergoes many elastic scattering events and a 'banana' shape (Feng *et al* 1995) characterizes the projections. This results in high correlation between the measurements and also is responsible for the low-resolution of DOT and a slow convergence of the algebraic inversion technique. Here, we investigated three different access orders. We will refer to them as systematic, sequential and random.

The systematic access scheme orders the measurement according to the order in which they are collected experimentally, namely by stepping the illumination source at adjacent spatial positions. This access order can be defined as $S_1D_1, S_1D_2, \ldots, S_1D_{N_d}, S_2D_1, \ldots, S_{N_s}D_{N_d}$.

The sequential access is used in a fan-beam configuration in CT without optimization. The projections are classified by groups of parallel beams and accessed group by group. In our case, we used the first data projection (S_1D_1) as the reference and all the other projections will be referenced by the angle between the line connecting the source–detector pair to the line connecting S_1D_1.

Finally, the random access is a randomization of all the measurements. This access is considered as the most efficient by van Dijke (van Dijke 1992).

2.5. Image quality evaluators

In order to evaluate the image quality achieved with each access order, we used common quantitative image evaluators. Four different evaluators were used in this study.

The first two evaluators are the correlation coefficient $\varepsilon_1^{(k)}$ and the root mean square error (Euclidian distance—$\varepsilon_2^{(k)}$) between the reconstruction and the model. The mathematical expressions of these coefficients are

$$\varepsilon_1^{(k)} = \frac{{}_i\,(t_i - \bar{t})\;\; x_i^{(k)} - \bar{x}^{(k)}}{{}_i\,(t_i - \bar{t})^2\;\; x_i^{(k)} - \bar{x}^{(k)}\;\;^2\Big]^{1/2}} \qquad \varepsilon_2^{(k)} = \left[\frac{{}_i\;\; x_i^{(k)} - t_i\;\;^2}{{}_i\,(t_i - \bar{t})^2}\right]^{1/2} \tag{3}$$

where $t_i\,(\bar{t})$ and $x_i^{(k)}\;\; \bar{x}^{(k)}$ each represents the pixel value (average value) in the original and kth reconstructed images, respectively. The correlation coefficient is more related to the accurate retrieval of the spatial distribution of the object function as the root mean square error is more related to the quantitative retrieval of the object function.

Another way to estimate the quality of the reconstruction is to compute the projection error $\varepsilon_3^{(k)}$ and the convergence rate $C_v^{(k+1)}$:

$$\varepsilon_3^{(k)} = \sum_i \left(\sum_j a_{ij} x_j^{(k)} - b_i \right)^2 \qquad C_v^{(k+1)} = \left[1 - \frac{\sum_i \left(\sum_j a_{ij} x_j^{(k+1)} - b_i \right)^2}{\sum_i \left(\sum_j a_{ij} x_j^{(k)} - b_i \right)^2} \right] \times 100. \quad (4)$$

The projection error measures the discrepancy between the data and their estimated values. The projection error is an indicator of the speed of the algorithm to recover the images. The convergence compares the difference between the measurements and the estimated measurements for two iterations. The convergence is often used as a criterion to stop the reconstruction. In other words, the convergence criterion, which controls the number of iterations used for the reconstruction, is the regularization parameter. In this perspective, the faster the numerical convergence criterion is reached, the better the reconstruction algorithm will be considered. In clinical applications where no *a priori* information are available, this parameter is used as the criterion of termination of the iterative process.

3. Results

The results of the reconstructions for the three access orders considered are shown in figure 2. For reconstruction purposes, the volume of interest was divided into 40×20 voxels. Only positive estimates were allowed in the iterative process.

Each frame of the sequence corresponds to a different iteration step that is shown in the title of each picture. The colour scale of the picture is normalized to the maximum of the random reconstruction at each iteration. The scale of the z-axis was fixed close to the maximum value of the model $\Delta\mu_a = 0.45\ \text{cm}^{-1}$. Figure 3 presents the value of different mathematical evaluators applied to the reconstructions of figure 2.

4. Discussion

As one can see from the sequence of figure 2, the use of different access orders leads to different reconstruction results for DOT. The differences are significant in the early iterations. The sequential and random accesses are showing two objects at the first iteration, however, the systematic access is giving a poor view of the spatial distribution of the object function. Moreover, the systematic access reconstructs large artefacts close to the boundaries. These artefacts correspond to the input order of the projections. Comparatively random and sequential access orders do not exhibit those artefacts. As the number of iterations increase, the three access orders are able to retrieve the two objects. They all become less sensitive to the boundary artefacts and give a good localization of the objects. Nonetheless, differences still exist between the three access orders. These differences are on the quantitative evaluation of the differential absorption. Random and sequential access orders estimate quantitatively the object function at the same pace. The main difference arises on the second object evaluation. On the other hand, at the same iteration number, the sequential access order always gives a lower estimation of the object function. This fact indicates that the random and the sequential access orders are faster to estimate properly the object function.

In an iterative process, the low-frequency components are recovered first and the high-frequency components are recovered later. Here the random and the sequential access orders are able to recover properly the low-frequency components from the first iteration. The correlation of the measurements in the systematic access order slows the recovery of the

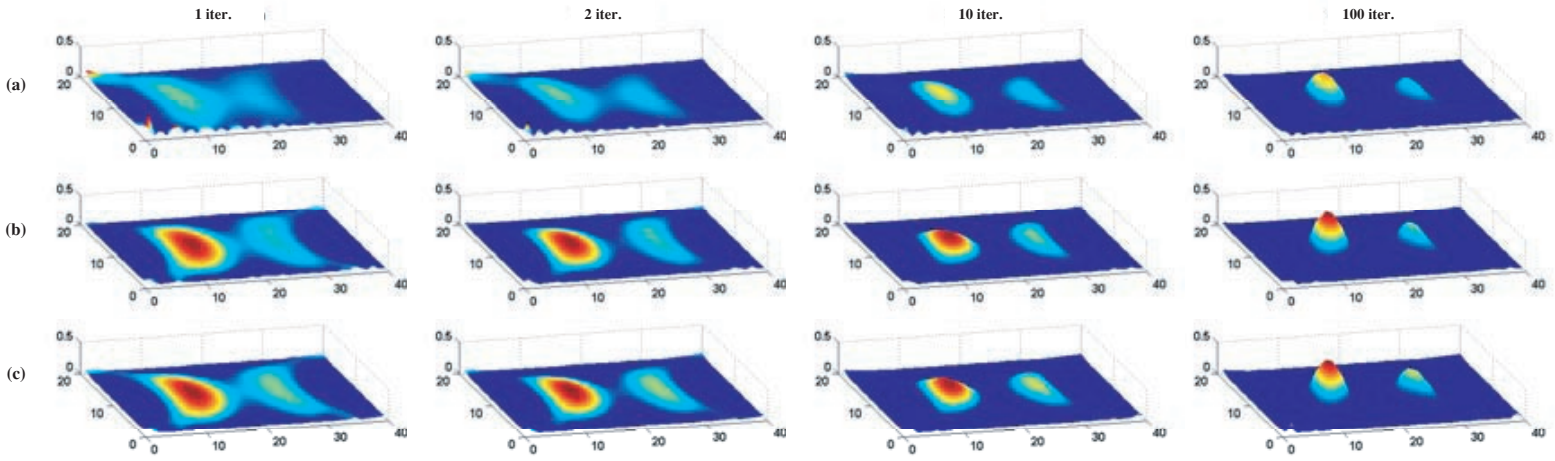

Figure 2. Reconstructions of the differential absorption at different iteration number for the three different access orders. The numbers of the iteration presented are given in the title of each sub-figure. The access orders are: (a) systematic, (b) sequential and (c) random.

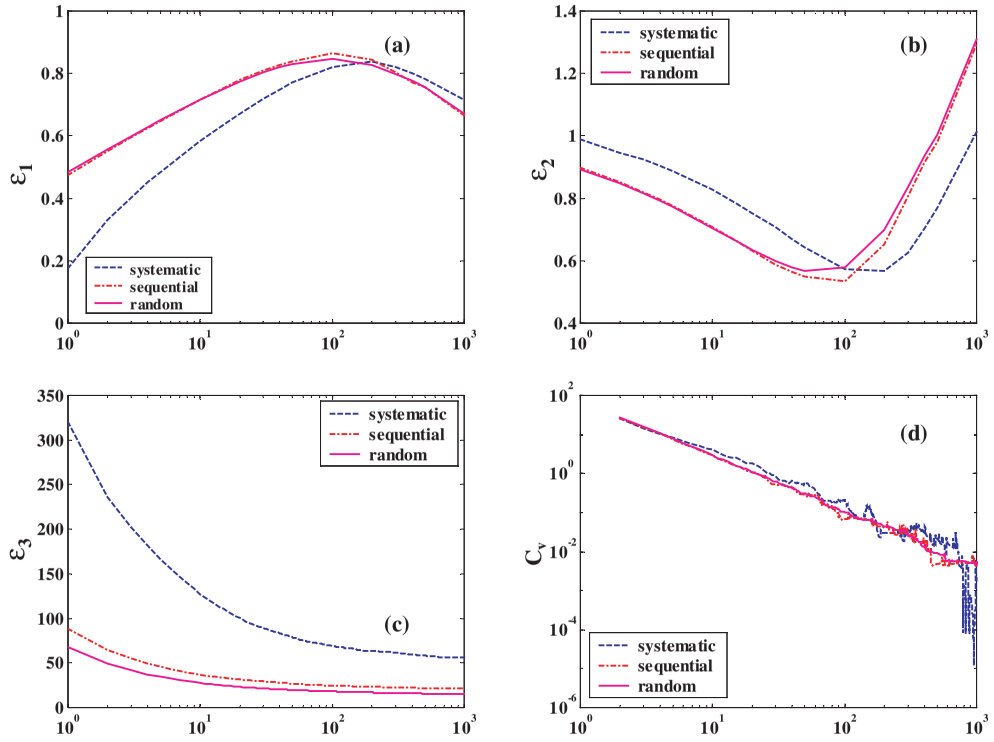

Figure 3. Mathematical evaluators for the reconstruction of figure 2. (a) Correlation coefficient, (b) Euclidian distance, (c) projection error and (d) convergence.

low-frequency components in the first stage of the ART algorithm. This correlation of the measurements still impacts on the late iterations.

The mathematical evaluators defined above enforced these findings. From ε_1 and ε_2 in figure 3(a) and (b), we notice that the entire image quality is affected by the access order used. The best reconstruction is obtained for the higher correlation coefficient and the lowest Euclidian distance. These two coefficients are congruent in figure 3. In the first step, the random access order is the scheme that leads to the better reconstruction relative to the two others. As the iterative process continues, the random and the sequential scheme come closer until the sequential access order outperforms the random access order. However, the best reconstructions are obtained for the same iteration numbers for the sequential and the random access orders. After this optimum reconstruction, the object function is overestimated. The correlation coefficient drops and the Euclidian distance rises. This effect of overestimation has already been reported by O'Leary (1996). It underlines the difficult problem of the choice of terminating the reconstruction. The systematic access order is slower to reach its optimum reconstruction. Moreover, the maximum value of the correlation coefficient and the minimum of the Euclidian distance are worse than the ones of the random and the sequential scheme indicating a globally poorer fidelity reconstruction.

From the study of ε_1 and ε_2, the sequential access order emerges as the best choice. However, it is not easy to assess the superiority of this scheme with the projection error or the convergence rate. In the case of ε_3, we see that the random access order has the lowest errors in fitting the measurements. It is also the most stable scheme regarding the convergence rate.

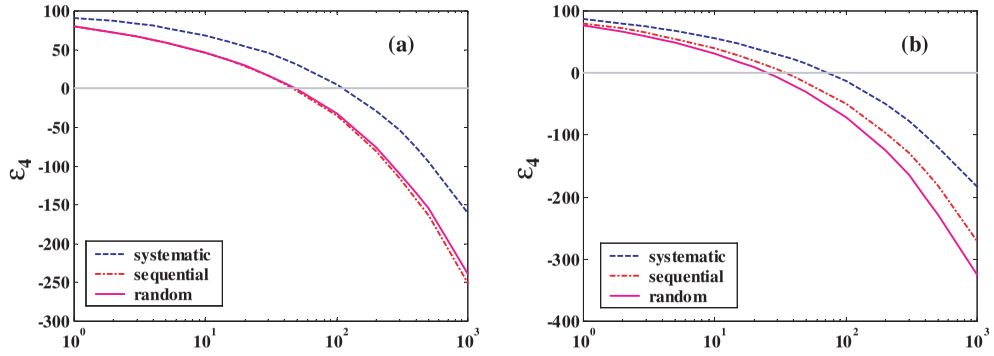

Figure 4. Fractional absorption errors estimation for (a) object of contrast 10 and (b) object of contrast 5 in reconstructions of figure 2 versus iterations.

The random and the sequential access orders outperformed the systematic scheme, but from these estimates, the random access order seems also to outperform the sequential access order in opposition to the findings using ε_1 and ε_2. Only the finding that random and sequential access orders outperformed the systematic order, is validated and these two access orders are *grosso modo* two times faster.

To have an idea of the quality of the reconstruction of the two objects, we calculate the fractional absorption error

$$\varepsilon_4^{(k)} = \left[1 - \frac{\Delta\mu_a^{(k)}}{\Delta\mu_a^{\text{model}}}\right] \times 100. \tag{5}$$

The results obtained from this evaluator are presented in figure 4. This evaluator has the advantage over ε_1 and ε_2 to discriminate the two object reconstructions. The best access order will be the one for which the fractional error is crossing the null-line for the closest iteration number for the two objects. We see that the sequential access order outperformed the two others when the second object is involved. In only considering the first object, the sequential and the random access orders produce similar estimation. The random access order is outperformed only when the second object is considered. The random access overestimates the object function of the second object when the first object function is chosen as a criterion (or ε_1 and ε_2).

However, we should note that we have considered the maximum of the object function with ε_4. For this reason, the best reconstructions are not found with ε_4 at the same iteration number as when using ε_1 and ε_2. The latest two are sensitive to the surface of the reconstructed object as ε_4 probes only the maximum of the reconstruction. Although, the conclusions drawn with ε_4 are considered valid and could be extrapolated for the global quality.

We also tested the three access orders with a random noise of 5% in amplitude and 0.5° on the measurements. This noise is more important than the noise related in the literature for existing optical imager. No important changes were recorded and the sequential access order still leads to the best reconstructions (results not shown here).

5. Conclusion

In this paper we investigated the impact of the projection access order in ART for DOT. The geometrical case considered was typical slab geometry with human breast optical values.

We have shown that the projection access order (when the number of projection is dense as when one use a CCD camera) affects both the speed to reach the best reconstructions and the quality of this reconstruction. Among the three access orders investigated herein, the sequential access order produced the optimal reconstruction compared to the model.

The differences between the three access orders investigated were important in the first iteration and for the retrieval of the object function of the lower contrast object. Those findings are important as ART is the most popular linear technique used to invert huge matrix in DOT. Thus, by selecting an appropriate access order, one is able to speed up the iterative reconstruction algorithm but also to reconstruct better image.

Moreover, considering appropriate access orders leads to a good estimation of the low-frequency components in the first iteration. This first iteration estimate that is fast to obtain could be used as *a priori* information for more refined image reconstruction such as zooming method (Jones *et al* 1997) for instance.

Acknowledgments

The authors are grateful to M Holboke for developing the finite difference code. They are also thankful to Mary Leonard for excellent drafting and Dot Coleman for text revisions. This work was supported in part by the National Institute of Health grant no CA 87046 and no R01-CA 60182-05.

References

Arridge S 1999 Optical tomography in medical imaging *Inverse Problems* **15** R41–R93

Culver J, Ntziachristos V, Zubkov L, Durduran T, Pattanayak D and Yodh 2000 A data set size and image quality in diffuse optical mammography; evaluation of a clinical prototype *Biomedical Topical Meetings, OSA Technical Digest* (Washington DC: Optical Society of America) pp 392–4

Durduran T, Holboke M, Culver J, Zubkov L, Choe R, Pattanayak D, Chance B and Yodh 2000 A Tissue bulk optical properties of breast and phantoms obtained with clinical optical imager *Biomedical Topical Meetings, OSA Technical Digest* (Washington DC: Optical Society of America) pp 386–8

Feng S, Zeng F-A and Chance B 1995 Photon migration in the presence of a single defect: a perturbation analysis *Appl. Opt.* **34** 3826–37

Gaudette R, Brook D, DiMarzio C, Kilmer M, Miller E, Gaudette T and Boas D 2000 A comparison study of linear reconstruction techniques for diffuse optical tomographic imaging of absorption coefficient *Phys. Med. Biol.* **45** 1051–70

Gordon R, Bender R and Herman G 1970 Algebraic reconstruction techniques for the three dimensional electron microscopy and X-Ray photography *J. Theor. Biol.* **69** 471–82

Guan H and Gordon R 1994 A projection access order for speedy convergence of ART: a multilevel scheme for computed tomography *Phys. Med. Biol.* **39** 2005–22

Guan H, Gordon R and Zhu Y 1998 Combining various projection access schemes with the algebraic reconstruction technique for a low-contrast detection in computed tomography *Phys. Med. Biol.* **43** 2413–21

Hawrys D and Sevick-Muraca E 2000 Developments toward diagnostic breast cancer imaging using near-infrared optical measurements and fluorescent contrast agents *Neoplasia* **2** 388–417

Haskell R, Svaasand L, Tsay TT, Feng Tc, McAdams M and Tromberg B 1994 Boundary conditions for the diffusion equation in radiative transfer *J. Opt. Soc. Am.* A **11** 2727–41

Herman G and Meyer L 1993 Algebraic reconstruction techniques can be made computationally efficient *IEEE Trans. Med. Imaging* **12** 600–9

Jones M, Proskurin S, Yamada Y and Tanikawa Y 1997 Application of the zooming method in near-infrared imaging *Phys. Med. Biol.* **42** 1993–2009

Kak A and Slaney M 1987 Computerized Tomographic Imaging (New York: IEEE Press)

Kaufman L 1992 Implementing and accelerating the EM algorithm for positron emission tomography *IEEE Trans. Med. Biol.* **37** 705–16

Matson C and Liu H 2000 Resolved object imaging and localization with the use of a backpropagation algorithm *Optics Express* **6** 168–74

Mueller K, Yagel R and Cornhill F 1997 The weighted-distance scheme: a globally optimizing projection ordering method for ART *IEEE Trans. Med. Imaging* **16** 223–30

Ntziachristos V and Chance B 2001 Probing physiology and molecular function using optical imaging: applications to breast cancer *Breast Cancer Res.* **3** 41–7

Ntziachristos V, Yodh A, Schnall M and Chance B 2000 Concurent MRI and diffuse optical tomography of breast after indocyanine green enhancement *Proc. Natl. Acad. Sci. USA* **97** 2767–72

O'Leary M 1996 Imaging with diffuse photon density waves *PhD Thesis* University of Pennsylvania

O'Leary M, Boas D, Chance B and Yodh 1995 A experimental images of heterogeneous turbid media by frequency-domain diffusing photon-tomography *Opt. Lett.* **20** 426–8

Ros D, Falcon C, Juvells I and Pavia J 1996 The influence of a relaxation parameter on SPECT iterative reconstruction algorithms *Phys. Med. Biol.* **41** 925–37

Shepp L and B Logan 1974 The Fourier reconstruction of a head section *IEEE Trans. Nucl. Sci.* **NS-21** 21–43

van der Sluis A and van der Vorst H 1990 SIRT- and CG-type methods for the iterative solution of sparse linear least-squares problems *Linear Algebra Appl.* **130** 257–302

van Dijke M 1992 Iterative methods in image reconstruction *PhD Thesis* Rijksuniversiteit Utrecht, The Netherlands

Villringer A and Chance B 1997 Non-invasive optical spectroscopy and imaging of human function *Trends Neurosci.* **20** 435–42

Yodh A and Chance B 1995 Spectroscopy and imaging with diffusing light *Phys. Today* **48** 34–40